IEEE Access
Multidisciplinary : Rapid Review : Open Access Journal

Received July 23, 2019, accepted August 8, 2019, date of publication August 12, 2019, date of current version August 27, 2019.

Digital Object Identifier 10.1109/ACCESS.2019.2934829

Precision Measurement Method of Laser Beams Based on Coordinate Measuring Machine

YUPENG LI[1,2], YA ZHAO[1,2], ZHI WANG[1], CHAO FANG[1], AND WEI SHA[1]
[1]Changchun Institute of Optics, Fine Mechanics and Physics, Chinese Academy of Sciences, Changchun 130033, China
[2]University of Chinese Academy of Sciences, Beijing 100049, China

Corresponding author: Wei Sha (sha_phe@163.com)

This work was supported by the Strategic Priority Research Program of the Chinese Academy of Science XDA1502070303 and the Youth Innovation Promotion Association of the Chinese Academy of Science under Grant 2019224.

ABSTRACT A high-precision stability measurement scheme was designed and prototyped with the purpose of ensuring precise laser beam alignment during the assembly of an integrated interferometer. With retroreflectors added, the angular resolution of the system is improved while ensuring system stability. Hydroxide-catalysis bonding technology is used to create a stress-free bond between the various optical components of the system. After calibration using the coordinate measuring machine, the device achieved a measurement accuracy of $\pm 6\ \mu$m for the absolute position of the laser beam in the global coordinate system. In angular measurements, an accuracy of $\pm 21\ \mu$rad was attained. Over a 2-month period, the maximum positional drifts and the maximum angular drifts of the calibration parameters were $\pm 3\ \mu$m and $\pm 27\ \mu$rad, respectively.

INDEX TERMS Laser beams, measurement, retroreflector, hydroxide-catalysis bonding, coordinate measuring machine, calibration.

I. INTRODUCTION

Being the technical device for acquiring gravitational wave scientific signals, the space laser interferometric ranging system is one of the most critical technologies in space gravitational wave detection [1]–[4]. To reduce the influence of system noise on measurement accuracy, the measurement platform requires an extremely precise alignment of the interference beam. With this objective, we proposed a sophisticated beam measurement system and assisted in the construction of the TaiJi Pathfinder interferometer, achieving a system stability of 6 pm/$\sqrt{\text{Hz}}$ [5]–[7].

The coordinate measuring machine (CMM) is a device enabling the geometry of physical objects to be transformed into CAD models. In the precision assembly process, this digital technology can accurately measure and obtain the size data but cannot independently complete measurements of the beam [8]–[10]. Conventional beam measurement devices (e.g., autocollimator, theodolite) are only able to determine the relative positional deviation between the interference beams [11]–[13], and are unable to complete measurements of the absolute position in the global coordinate system. The measurement system proposed by Fitzsimons and collaborators achieves a higher absolute measurement accuracy [14], [15], but the installation of plane reflectors (single-sided mirrors) and the use of traditional epoxy glue for bonding means the calibration parameters drift significantly over time.

We propose a calibrated spatial-beam positioning system (SPS), in which the retroreflectors (double-sided mirrors, Figure 2) and hydroxide-catalysis bonding [15]–[17] are used. The retroreflectors magnify the angular deviation of the system by folding the optical path, thereby improving the angular resolution of the detection. Simultaneously, the unique beam transfer performance of the retroreflector combined with the low-stress hydroxide-catalysis bonding method improves the stability of the system considerably. Based on the CMM, calibrated SPS can measure the absolute position of the beam in the global coordinate system. Finally, the experimental results show that the measurement accuracy of the beam position parameters under the global coordinate system is $\pm 6\ \mu$m and $\pm 21\ \mu$rad, and the drift of the calibration parameters of the prototype is only $\pm 3\ \mu$m and $\pm 27\ \mu$rad over a 2-month period at a temperature of 22$\pm$0.5°C in the laboratory.

II. MEASURING PRINCIPLE

The measurement principle of the SPS is to capture a unique laser beam through two quadrant photodiodes (QPDs, Figure 2). For a beam passing through two quadrant

The associate editor coordinating the review of this article and approving it for publication was Wei Liu.

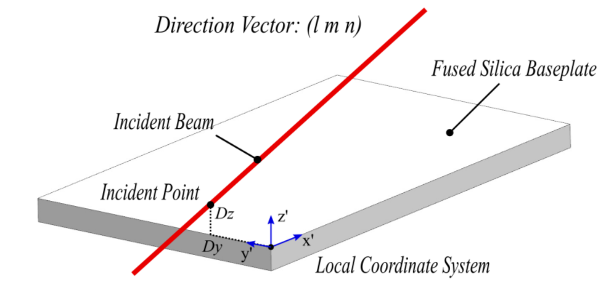

FIGURE 1. Relative positional relationship between beam and baseplate in the local coordinate system.

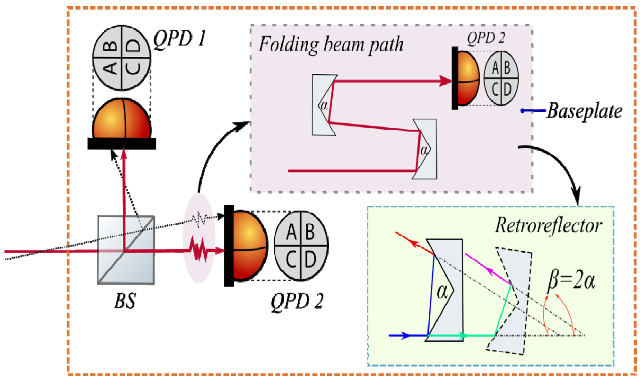

FIGURE 2. Schematic diagram of system composition.

photodiode centers at the same time, particular position parameters exists with respect to the SPS baseplate, i.e., the incident point (0, Dy, Dz) and the directional vector (l, m, n) of the beam are constant in the local coordinate system (Figure 1). Then based on CMM, the beam parameters can be obtained by calibration.

The local coordinate system is usually built on the front end of the SPS baseplate and must maintain a constant position during calibration and use. In the local coordinate system, the beam traces a linear path, expressed mathematically as

$$\frac{x'}{l} = \frac{y' - Dy}{m} = \frac{z' - Dz}{n}. \tag{1}$$

The system (Figure 2) consists of a front-end beam splitter, retroreflectors, and back-end QPDs. The formula for calculating the angular resolution ω of the system simplifies,

$$\omega = \frac{D}{L}. \tag{2}$$

where D is the position resolution of the QPD, and L is the optical path difference between the beam reaching different detectors after the BS.

Folding the optical path increases the back-end optical path and is an effective way to increase the angular resolution of the system. In our proposal, retroreflectors are used to replace the plane reflectors in the conventional scheme. Hence the angle between the outgoing light and the incident light is no longer dependent on the angle of incidence, but only depends on the angle α of the retroreflector. With this advantage, the angle accuracy of the system is not affected when the position of the reflector changes through the expansion and shrinking of the glue layer or by external disturbances, although the position accuracy slightly diminishes (Figure 2).

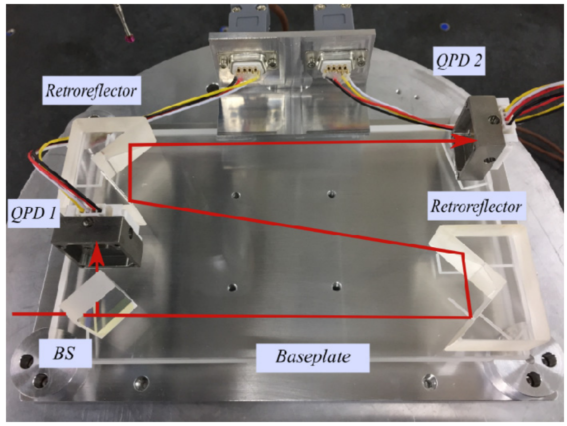

FIGURE 3. Physical diagram of the retroreflector SPS prototype.

III. SYSTEM DESIGN

The optical elements of the completed retro-reflector SPS prototype (Figure 3) are made of fused silica, and the metal supports of the QPDs are of invar steel with a coefficient of linear expansion matching that of fused silica. Fused silica glass has an ultra-low coefficient of linear expansion coefficient whereas invar steel has sufficient structural stability, which mitigates background disturbances on the measurement system. The QPD uses INGAAS material, which has higher responsiveness to the 1064-nm wavelength laser required for gravitational wave detection [2].

The optical components in the system are bonded to the baseplate using the hydroxide-catalysis bonding technique. The adhesive solution is prepared by diluting 14% NaOH and 27% SiO_2 silicate solution with deionized water in a 1:6 ratio. To improve reliability, bonding was completed in a Class 100 clean room, and the flatness of the component bonding surface was within $\lambda/10$ ($\sim$60 nm, $\lambda = 632.8$ nm). Compared with the conventional bonding method using optical epoxy adhesive, the bond not only has sufficient strength, but its adhesive layer is also very thin with a thickness of $\sim$100 nm [17], [18]. With a very low bonding stress, the layer moreover reduces effectively the impact of background disturbances on the positional accuracy of components.

IV. ERROR ANALYSIS

A. MEASURING ERROR OF THE CMM

The calibration of the SPS requires an auxiliary measurement obtained by the CMM, which has a position accuracy of 1.5 μm + 1 μm/m; the angular error also improves with increased measurement length. Taking into account its measurement accuracy and processing difficulty, the length of the SPS baseplate was set at 220 mm. In this measurement range, the CMM position accuracy is approximately 2 μm and the angular accuracy is about 8–10 μrad.

B. DETECTOR RESOLUTION

The spatial position of the beam is locked by two QPDs on the SPS. The optical path length between the two QPDs is the optical path difference between the two beams passing through the BS, and is about 500 mm. The QPD used has a resolution of ± 1 μm, resulting in an angular error of approximately 3–5 μrad. If the folded optical path is removed (the optical path difference changes to approximately 120 mm), the alignment efficiency of the system improves, but the measurement accuracy is reduced to 13–21 μrad.

Therefore, the uncertainty errors caused by measuring equipment (CMM and QPDs) are about 1-3μm and 5-15μrad.

C. ENVIRONMENTAL DISTURBANCE

Affected by factors such as bonding stress, temperature fluctuation, and environmental vibration, the system undergoes a certain degree of deformation and causes the calibration parameters to drift with time. Our evaluation of this drift integrates finite-element-analysis software HYPERMESH and optical design software CODE V, to analyze the deviation of the beams under gravity and temperature fluctuation conditions. From the analysis results, the offset of the spot on QPD 1 and QPD 2 of the retroreflector system with the hydroxide-catalysis bonding is -2 μm and 5 μm when the system is in the horizontal state and the temperature fluctuation is maintained within ± 0.5°C. However, the offset of the spot on the QPD of the plane-reflector system with epoxy adhesive is -6 μm and 120 μm. Therefore, the retro-reflector SPS system offers a more stable system performance.

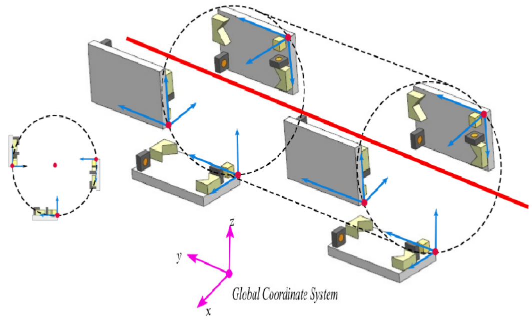

a) Calibration schematic diagram

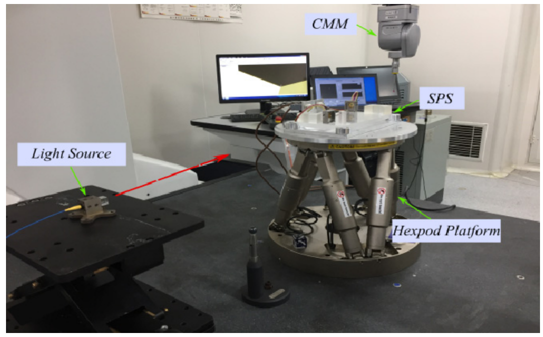

b) calibration test sites

FIGURE 4. (a) Schematic of the calibration scheme principles and (b) photograph of the calibration test set-up. During calibration, the space beam passes through the SPS and incidents the centers of the two detectors simultaneously. The CMM is used for auxiliary measurements. The hexapod platform is used for posture adjustments.

V. CALIBRATION PROCESS

For calibrations (see Figure 4), the global coordinate system is the reference coordinate system of the CMM. The local coordinate system is established on the SPS and is used to determine the spatial position of the SPS. Once the global and local coordinate systems are determined, calibration begins with the following three steps [14], [19]:

1) Moving alignment: the SPS is aligned with an ultra-stable calibration beam, then rotated and shifted around the beam by means of a hexapod platform, and keeps the beam aligned (the number shown on two QPDs is 0) throughout the movement process. In the process, the origin $\left(x_0', y_0', z_0'\right)$ of the local coordinate system under the global coordinate system and its unit coordinate vector $\left(u_x', u_y', u_z'\right)$ will be recorded by the CMM, for which

$$u_x' = (u_{x1}', u_{x2}', u_{x3}'), \tag{3}$$
$$u_y' = (u_{y1}', u_{y2}', u_{y3}'), \tag{4}$$
$$u_z' = (u_{z1}', u_{z2}', u_{z3}'). \tag{5}$$

2) Beam fitting: ideally, origin of each local coordinate system would be roughly distributed on a cylindrical surface centered along the beam axis, then the spatial position of the beam under the global coordinate system is fitted by the three-dimensional CMM.

3) Solution by coordinate transformation: the position parameters of the beam under the local coordinate system are solved by the position transformation of the point. The transformation formula for the point (x_i, y_i, z_i) of the space line under the global coordinate system to the local coordinate system points $\left(x_i', y_i', z_i'\right)$ is

$$\left(x_i', y_i', z_i', 1\right) = (x_i, y_i, z_i, 1) \cdot T \cdot R. \tag{6}$$

where the coordinate rotation matrix in the augmented-matrix form being set to

$$R = \begin{bmatrix} u_{x1}' & u_{y1}' & u_{z1}' & 0 \\ u_{x2}' & u_{y2}' & u_{z2}' & 0 \\ u_{x3}' & u_{y3}' & u_{z3}' & 0 \\ 0 & 0 & 0 & 1 \end{bmatrix}; \tag{7}$$

and the translation matrix being

$$T = \begin{bmatrix} 1 & 0 & 0 & 0 \\ 0 & 1 & 0 & 0 \\ 0 & 0 & 1 & 0 \\ -x_0' & -y_0' & -z_0' & 1 \end{bmatrix}. \tag{8}$$

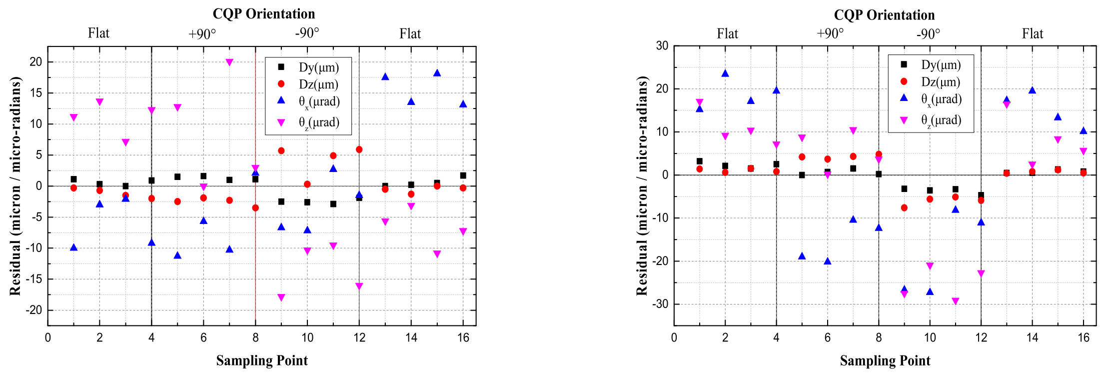

a) Retro-reflector system measurement accuracy

b) Plane-reflector system measurement accuracy

FIGURE 5. Measurement accuracy of (a) the retro-reflector and (b) the plane-reflector systems, the horizontal coordinates represent sampling points in different directions, and the longitudinal coordinates are expressed as deviations between actual measured values and fitted values, i.e., the residual difference.

Therefore, the equation of the space line under the local coordinate system is

$$\frac{x'-x'_1}{x'_2-x'_1}=\frac{y'-y'_1}{y'_2-y'_1}=\frac{z'-z'_1}{z'_2-z'_1}. \tag{9}$$

From this equation, the point $(0, Dy, Dz)$ and the directional vector (l, m, n) of the beam under each local coordinate system are solved. When SPS is used, the CMM is still needed to establish the local and global coordinate systems. From the known calibration parameters, the beam coordinates are expressed in the reference coordinate system, and then the position of the beam in the global coordinate system is obtained by the coordinate transformation.

In data analysis, directional vectors are usually given in terms of the angle between the beam and the axes to establish the angular accuracy of the calibration parameters. where the angle between the beam and the x, z axis is given by

$$\theta_x = arc\cos\frac{l}{\sqrt{l^2+m^2+n^2}}, \tag{10}$$

$$\theta_z = arc\cos\frac{n}{\sqrt{l^2+m^2+n^2}}. \tag{11}$$

VI. RESULTS AND DISCUSSIONS

The performance evaluation of SPS is performed regarding two aspects, one being accuracy and the other stability of the calibration parameters over long periods, i.e., repeatability.

The fitting of the calibration parameters requires at least three directions and five measuring points. To increase the reliability of the data, in the actual calibration process, the number of sample points n is taken to be 16, and a large angle deflection range of 0° and ±90° is chosen. The final direction of the calibration is set to the same direction as the initial angle (flat) to verify the validity of the previous data and whether the calibration beam moves during the calibration process.

After calibration, the average value $\overline{X}$ of the measurements $X_i\,(Dy, Dz, \theta_x, \theta_z)$ is taken as the optimal estimate of the calibration parameters, which is (17.1752, 11.54, 3.1389298, 1.5718590). The uncertainty (i.e., confidence interval estimation) of the calibration parameters is obtained from [20]

$$\delta_X = \pm t_p\,(f)\cdot\sigma\big/\sqrt{n}, \tag{12}$$

where σ is the standard deviation of the experiments, which is obtained using the Bessel formula,

$$\sigma=\sqrt{\frac{1}{n-1}\sum_{i=1}^{n}v_i^2}=\sqrt{\frac{1}{n-1}\sum_{i=1}^{n}\left(X_i-\overline{X}\right)^2}, \tag{13}$$

with freedom $f = n-1$. A plot of typical residuals for a retroreflector SPS calibration is given in Figure 5a. Taking the maximum residual value as the half-bandwidth of $p = 99.9\%$, we then check the t-distribution table to find $t_{0.999}\,(15) = 4.073$ [21]. Hence, the uncertainties of the calibration parameters δ_X is (±1.6 μm, ±3 μm, ±10.4 μrad, ±12 μrad), which reflects the smaller dispersion of the calibration parameters under repetitive conditions.

The residuals give an estimation of the accuracy. The maximum residual v_{max} reflects the limit distribution state of measurement error and is used to express the measurement accuracy. To validate the performance advantages of the retro-reflector system, the experimental results are compared with those of our previous plane-reflector system with epoxy adhesive bonding. As is seen in Figure 5, the measurement accuracies of the retro-reflector and plane-reflector systems after calibration were ±6 μm, ±21 μrad and 8 μm, ±29 μrad, respectively.

The stability of the calibration parameters is another key indicator of the performance of the device that determines whether the device needs to be recalibrated for subsequent use. For this reason, we monitored the calibration parameters of the system over a 2-month period. Table 1 shows a comparison of the calibration parameter fluctuations before and after 2 months. Over a 2-month period, the respective deviation in the calibration parameters from their initial values were ±3 μm, ±27.1 μrad and ±11.3 μm, ±234 μrad. The exact source of the stability error is unknown, but there are strong

TABLE 1. Calibration parameters and stability of retro-reflector and plane-reflector system.

Root-Mean-Square	D_y	D_z	θ_x	θ_z
Plane-reflector	17.1752 mm	11.5400 mm	3.1389298	1.5718590
Plane-reflector-2month	17.1794 mm	11.5290 mm	3.1388303	1.5720859
Differentials	4.2 μm	-11.3 μm	102.6 μrad	-234 μrad
Retro-reflector	15.1285 mm	11.5577 mm	3.1246267	1.568844
Retro-reflector-2month	15.1296 mm	11.5607 mm	3.1246112	1.5688177
Differentials	1.1 μm	3 μm	16 μrad	27.1μrad

indications that this is may be due to movements in the reflectors.

Comparing the two schemes, the measurement accuracy was found to be basically the same after the calibration, but the retro-reflector system offers a greater stability over time. That is, the retro-reflector system effectively avoids the shortcomings of the older system which needed to be calibrated repeatedly when used, and helps in improving the actual efficiency of use.

VII. CONCLUSION AND OUTLOOK

A position measurement system of a space laser beam is described and introduced in detail in regard to its measuring principle, calibration scheme, and error analysis. An experimental comparison between conventional systems highlights the necessity to resolve the positioning problem of laser beams. We used retroreflectors and the hydroxide-catalysis bonding technique to improve the system in terms of measurement accuracy and system stability. After calibration, the device meets the requirements of ± 10 μm and ± 50 μrad for position and angle measurement accuracy for the Taiji pathfinder mission. Benefiting from the use of SPS, the sensitivity of the optical bench of the Taiji pathfinder prototype has reached 6 pm/$\sqrt{}$Hz in the frequency band from 0.03 Hz to 1 Hz. Next, to meet the needs of higher-precision missions, the measurement accuracy of the SPS can be improved by increasing the measurement accuracy of the CMM, optimizing the measurement method, and increasing the error resolution of the detector by adding a magnifying lens assembly.

REFERENCES

[1] Z. R. Luo *et al.*, "Space laser interferometry gravitational wave detection," *Adv. Mech.*, vol. 43, no. 4, pp. 415–447, 2013.

[2] P. Amaro-Seoane *et al.*, "Laser interferometer space antenna," Feb. 2017, *arXiv:1702.00786*. [Online]. Available: https://arxiv.org/abs/1702.00786

[3] S. L. Danilishin, E. Knyazev, N. V. Voronchev, F. Y. Khalili, C. Gräf, S. Steinlechner, J.-S. Hennig, and S. Hild, "A new quantum speed-meter interferometer: Measuring speed to search for intermediate mass black holes," *Light, Sci. Appl.*, vol. 7, no. 1, p. 11, 2017.

[4] S. Vitale, "Space-borne gravitational wave observatories," *General Relativity and Gravitation*, vol. 46, p. 1730, May 2014.

[5] H. Liu, Y. Dong, R. Gao, Z. Luo, and G. Jin, "Principle demonstration of the phase locking based on the electro-optic modulator for Taiji space gravitational wave detection pathfinder mission," *Opt. Eng.*, vol. 57, no. 5, 2018, Art. no. 054113.

[6] Y. Li, H. Liu, Y. Zhao, W. Sha, Z. Wang, Z. Luo, and G. Jin, "Demonstration of an ultraprecise optical bench for the Taiji space gravitational wave detection pathfinder mission," *Appl. Sci.*, vol. 9, no. 10, p. 2087, 2019.

[7] Z. Luo, H. Liu, and G. Jin, "The recent development of interferometer prototype for Chinese gravitational wave detection pathfinder mission," *Optics Laser Technol.*, vol. 105, pp. 146–151, Sep. 2018.

[8] M. Ren, L. Kong, L. Sun, and C. Cheung, "A curve network sampling strategy for measurement of freeform surfaces on coordinate measuring machines," *IEEE Trans. Instrum. Meas.*, vol. 66, no. 11, pp. 3032–3043, Nov. 2017.

[9] Y. Wang, P. Su, R. E. Parks, C. J. Oh, and J. H. Burge, "Swing arm optical coordinate-measuring machine: High precision measuring ground aspheric surfaces using a laser triangulation probe," *Opt. Eng.*, vol. 51, no. 51, 2015, Art. no. 073603.

[10] R. D'Amato, J. Caja, P. Maresca, and E. Gómez, "Use of coordinate measuring machine to measure angles by geometric characterization of perpendicular planes. Estimating uncertainty," *Measurement*, vol. 47, no. 1, pp. 598–606, 2014.

[11] Y.-L. Chen, Y. Shimizu, J. Tamada, Y. Kudo, S. Madokoro, K. Nakamura, and W. Gao, "Optical frequency domain angle measurement in a femtosecond laser autocollimator," *Opt. Express*, vol. 25, no. 14, pp. 16725–16738, 2017.

[12] K. Li, C. Kuang, and X. Liu, "Small angular displacement measurement based on an autocollimator and a common-path compensation principle," *Rev. Sci. Instrum.*, vol. 84, no. 1, 2013, Art. no. 015108.

[13] J. Luo, Z. Wang, Z. Wen, M. Li, S. Liu, and C. Shen, "Reflector automatic acquisition and pointing based on auto-collimation theodolite," *Rev. Sci. Instrum.*, vol. 89, no. 1, 2018, Art. no. 015101.

[14] E. D. Fitzsimons, J. Bogenstahl, J. Hough, C. J. Killow, M. Perreur-Lloyd, D. I. Robertson, and H. Ward, "Precision absolute positional measurement of laser beams," *Appl. Opt.*, vol. 52, no. 12, pp. 2527–2530, 2013.

[15] C. J. Killow, E. D. Fitzsimons, J. Hough, M. Perreur-Lloyd, D. I. Robertson, S. Rowan, and H. Ward, "Construction of rugged, ultrastable optical assemblies with optical component alignment at the few microradian level," *Appl. Opt.*, vol. 52, no. 2, pp. 177–181, 2013.

[16] K. Haughian, R. Douglas, A. A. van Veggel, J. Hough, A. Khalaidovski, S. Rowan, T. Suzuki, and K. Yamamoto, "The effect of crystal orientation on the cryogenic strength of hydroxide catalysis bonded sapphire," *Classical Quantum Gravity*, vol. 32, no. 7, 2015, Art. no. 075013.

[17] K. Haughian, D. Chen, L. Cunningham, G. Hofmann, J. Hough, P. G. Murray, R. Nawrodt, S. Rowan, A. A. van Veggel, and K. Yamamoto, "Mechanical loss of a hydroxide catalysis bond between sapphire substrates and its effect on the sensitivity of future gravitational wave detectors," *Phys. Rev. D, Part. Fields*, vol. 94, no. 8, 2016, Art. no. 082003.

[18] E. J. Elliffe, J. Bogenstahl, A. Deshpande, J. Hough, C. Killow, S. Reid, D. Robertson, S. Rowan, H. Ward, and G. Cagnoli, "Hydroxide-catalysis bonding for stable optical systems for space," *Classical Quantum Gravity*, vol. 22, no. 10, pp. S257–S267, 2005.

[19] C. J. Killow, E. D. Fitzsimons, M. Perreur-Lloyd, D. I. Robertson, H. Ward, and J. Bogenstahl, "Optical fiber couplers for precision spaceborne metrology," *Appl. Opt.*, vol. 55, no. 10, pp. 2724–2731, 2016.

[20] W. Bich, M. G. Cox, and P. M. Harris, "Evolution of the 'guide to the expression of uncertainty in measurement,'" *Metrologia*, vol. 43, no. 4, p. S161, 2006.

[21] L. Kirkup, *An Introduction to Uncertainty in Measurement: Using the GUM* (Guide to the Expression of Uncertainty in Measurement). Cambridge, U.K.: Cambridge Univ. Press, 2006.

[22] R. R. Wilcox and G. A. Rousselet, "A Guide to Robust Statistical Methods in Neuroscience," *Current Protocols Neurosci.*, vol. 82, no. 1, pp. 8.42.1–8.42.30, 2018.

[23] J. Qin, R. M. Silver, B. M. Barnes, H. Zhou, R. G. Dixson, and M.-A. Henn, "Deep subwavelength nanometric image reconstruction using Fourier domain optical normalization," *Light, Sci. Appl.*, vol. 5, Feb. 2016, Art. no. e16038.

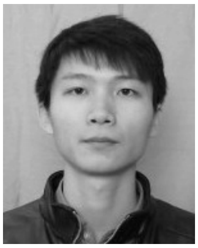

YUPENG LI received the B.S. degree from the Qingdao University of Science & Technology, China, in 2015. He is currently pursuing the Ph.D. degree with the Changchun Institute of Optics, Fine Mechanics and Physics, Chinese Academy of Science. His current research interest includes optical-mechanical structure design and simulation.

YA ZHAO received the B.S. degree from Northeastern University, China, in 2016. He is currently pursuing the Ph.D. degree with the Changchun Institute of Optics, Fine Mechanics and Physics, Chinese Academy of Science. His current research interests include optical design and simulation, and interferometric systems.

ZHI WANG received the B.S. and the M.Sc. degrees in mechanical engineering from the Changchun University of Science and Technology, in 1985 and 1988, respectively, and the Ph.D. degree in optical engineering from CIOMP, in 1998. He is currently the Vice-Director of the State Key Laboratory of Applied Optics, CIOMP, CAS. His research interests include design and manufacturing of space telescope and interferometric systems.

CHAO FANG was born in Huainan, Anhui, China, in 1985. He received the B.S. and M.S. degrees in optical engineering from Tianjin University, in 2007 and in 2009, respectively, and the Ph.D. degree in optics from the Changchun Institute of Optics, Fine Mechanics and Physics, Chinese Academy of Science, in 2018, where he has been a Research Associate with the State Key Laboratory of Applied Optics, since 2011. From 2009 to 2011, he was a Research Assistant with the State Key Laboratory of Applied Optics, Changchun Institute of Optics, Fine Mechanics and Physics, Chinese Academy of Science.

WEI SHA was born in Tianjin, China. He received the B.S. degree from Shanghai Jiaotong University, in 2007, and the Ph.D. degree from the Changchun Institute of Optics, Fine Mechanics and Physics, Chinese Academy of Science, in 2012. His research interests include optical-mechanical structure design and engineering analysis of space telescope.